Rotating Chemical Waves in Small Circular Domains

N. Hartmann,[1] M. Bär,[1,2] I. G. Kevrekidis,[2] K. Krischer,[1] and R. Imbihl[3,*]

[1]*Fritz-Haber-Institut der Max-Planck-Gesellschaft, Faradayweg 4-6, D-14195 Berlin, Germany*

[2]*Department of Chemical Engineering, Princeton University, Princeton, New Jersey 08544-5263*

[3]*Institut für Physikalische Chemie und Elektrochemie, Universität Hannover, Callinstrasse 3-3A, D-30167 Hannover, Germany*

(Received 28 September 1995)

The influence of the domain size on the properties of rotating waves in the NO + CO reaction on a microstructured Pt(100) surface is investigated for circular geometries. Below a critical domain size, determined by the spiral wavelength in an unbounded medium, the frequency of the rotating waves increases substantially due to interaction of the wave tip with the boundary. The phenomena are reproduced qualitatively with a reaction-diffusion model.

PACS numbers: 82.65.Jv, 05.70.Ln

Pattern formation in reaction-diffusion systems has been studied mainly in situations where the boundaries do not play an important role. In many cases, essential quantities like the wavelength and temporal period of a pattern are unchanged by the actual system geometry. One ubiquitous pattern in experiments and models is a rotating spiral wave [1–3] which in the simplest case performs a rotation with a unique, parameter-dependent frequency around a localized core region. Recently, it was shown that the presence of the boundary can affect the propagation of reaction-diffusion waves in a crucial manner: New spirals may form when plane waves encounter sharp corners in a boundary [4], while existing spirals tend to drift along the boundaries [5,6]. However, as has been demonstrated in a few theoretical studies, not only the geometry [7] but also the size of the domain influences properties and existence of these patterns [8].

Here we present experiments on a pattern-forming reaction in small circular domains of varying sizes. While spiral waves appear under our experimental conditions in larger domains, rotating "pulses" are observed for the same control parameters in these small circles (they may be interpreted as spiral tips). The properties of these waves change drastically as the diameter of the domains becomes comparable to the spiral wavelength in large, practically unbounded domains. The experiments are complemented by numerical simulations showing the scaling behavior of the period with respect to the domain size and the influence of the parameters.

The system studied is the NO + CO reaction on a microstructured Pt(100) surface. We investigate the reaction under isothermal conditions at low pressure (10^{-6} mbar range). From previous studies it is well known that the reaction exhibits spiral waves and wave trains whose wavelength varies strongly with temperature [9]. Using microlithographic techniques, we constructed small circular domains of the bare Pt surface which are surrounded by an inert layer of Ti/TiO_2 [10]. The size of the catalytically active domains (20–400 μm) is the range of the wavelength of the patterns. The spatiotemporal dynamics of the adsorbate concentration (or more precisely the local work function change) are recorded with a photoemission electron microscope (PEEM) permitting a spatial resolution of ≈ 1 μm and a temporal resolution of 20 ms [11].

Figure 1(a) displays a PEEM image in a 200 μm circle recorded under conditions where the ratio wavelength/domain size of 40 μm/200 μm still allows a clear identification of a spiral pattern. In the small domains of 20, 30, 40, and 50 μm size the visual impression is that of a rotating pulse, but a reliable assignment of the pattern re-

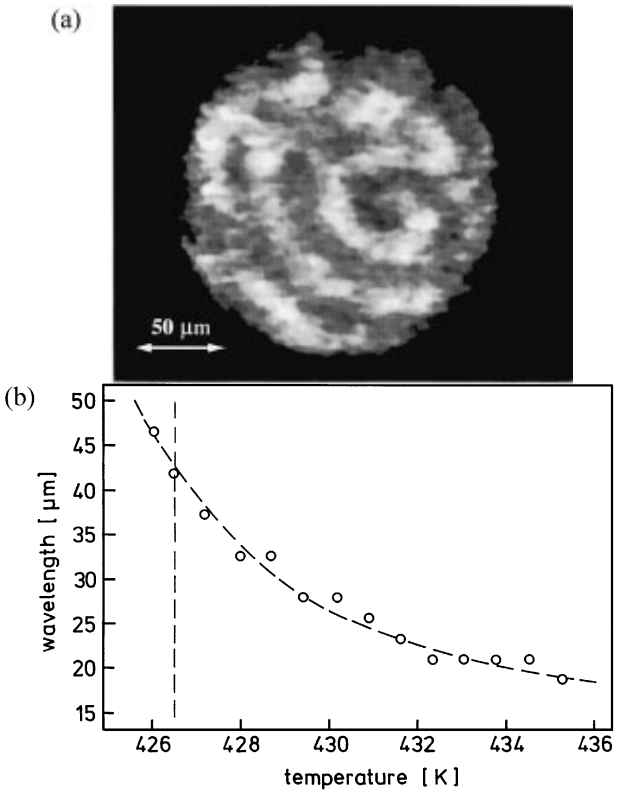

FIG. 1. Spiral waves in large circular domains of Pt(100) in the NO + CO reaction. Experimental conditions: $p_{NO} = 4 \times 10^{-6}$ mbar, $p_{CO} = 3 \times 10^{-6}$ mbar. (a) PEEM image recorded at $T = 426.5$ K showing a spiral wave in a 200 μm circular domain. (b) Dependence of the wavelength λ on the sample temperature T. The data were measured in a 400 μm circle.

 0031-9007/96/76(8)/1384(4)$06.00

quires a more elaborate analysis as will be shown below. Spiral waves are found in a temperature range between 426 and 436 K for the chosen p_{NO}, p_{CO} conditions. Figure 1(b) shows the dependence of the spiral wavelength on the surface temperature as measured in the 400 μm circle. The temperature at which the following measurements have been performed is marked by a dashed line. The strong increase of the wavelength at the low temperature boundary of the spiral region is characteristic for excitable media [3].

Measurements of the local intensity variations by integrating the PEEM intensity in a small window of 5×5 μm size yields the time series displayed in Fig. 2. The frequency ν increases considerably with decreasing domain size as evidenced by a ratio $\nu_{50} : \nu_{40} : \nu_{30} : \nu_{20} \approx 1 : 1 : 2 : 3$. Such a strong dependence of the frequency on the domain size was, however, observed only when p, T conditions were chosen close to the boundary of the existence range for spiral waves.

For a careful analysis of the patterns in the small domains, the method of empirical orthogonal eigenfunctions (EOF) or Karhunen-Loeve (KL) decomposition was applied to the spatiotemporal data [12,13]. This method is widely used for the identification of coherent spatial structures from experimental or numerical spatiotemporal data [14]. The procedure extracts the main components of the dynamics in the form of linearly independent orthogonal eigenfunctions which are optimal in the sense that the overlap of the data with the eigenfunctions is maximized for a given number of modes. Hence, the spatiotemporal data $u(\mathbf{r}, t)$ in this method are represented in the form $u(\mathbf{r}, t) = \sum_i a_1(t)\psi_i(\mathbf{r})$ with ψ_i denoting spatial mode i and $a_i(t)$ the time-dependent coefficient of mode i. The KL method also has the advantage that it discerns the dominant structures in the presence of a strong background noise.

The KL decomposition of the four cycles (20, 30, 40, and 50 μm diameter) yielded similar modes and, for this reason, only the important EOFs of the 40 μm circle are displayed in Fig. 3(a). For comparison, the corresponding EOFs of a simulated rotating wave are shown in Fig. 3(b). Due to the influence of surface structural defects in our data, the observed and calculated ordering of the modes do not coincide. All the modes shown in Fig. 3 are complemented by partner modes with comparable weight that are rotated by angles of $\pi/2$, $\pi/4$, and $\pi/6$, respectively. A similar behavior is found for the time-dependent coefficients $a_i(t)$ of such a pair; they are shifted by a quarter of their period. Thus the reconstruc-

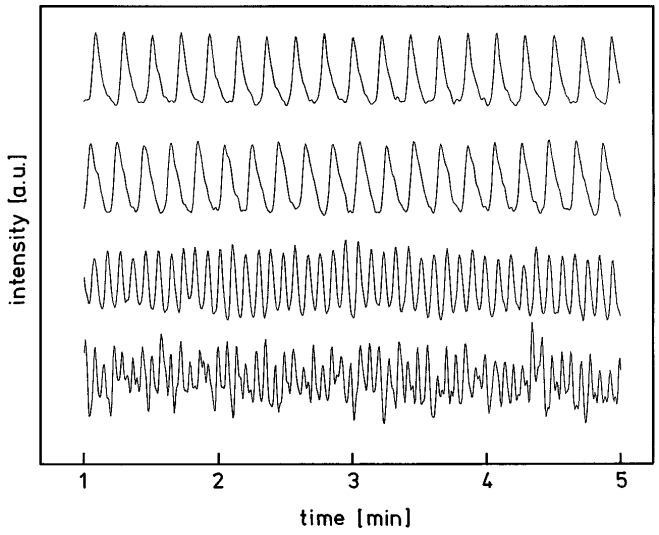

FIG. 2. Local PEEM intensity variations in domains of 20, 30, 40, and 50 μm diameter (from bottom to top). The PEEM intensity was integrated in a window of 5×5 μm size in each case. Experimental conditions: $T = 426.5$ K, $p_{NO} = 4 \times 10^{-6}$ mbar, $p_{CO} = 3 \times 10^{-6}$ mbar. All data shown have been scaled to the same maximum amplitude.

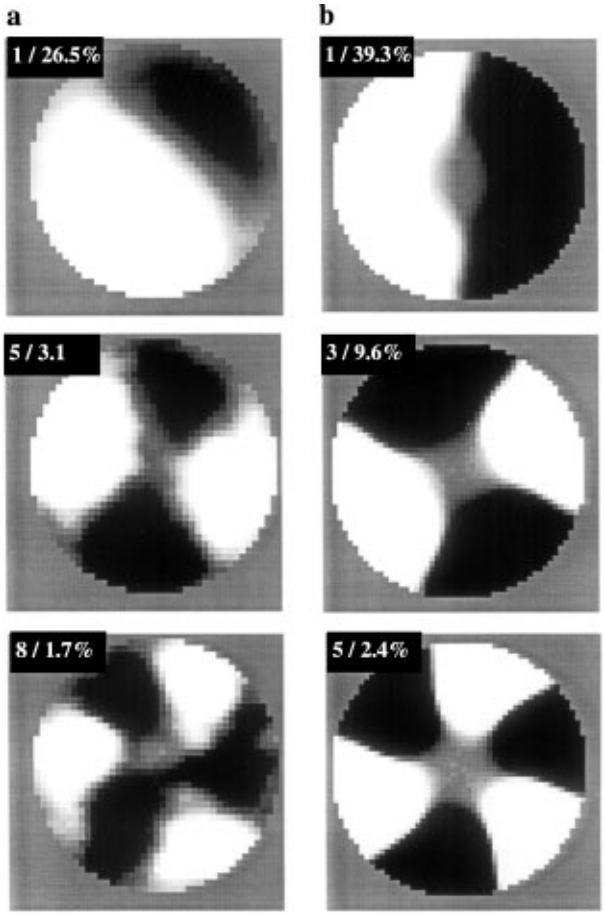

FIG. 3. (a) Comparison of a KL decomposition of experimental data and (b) a simulated spiral wave. The number and the weight are given for each mode. The experimental data were taken from the 40 μm circle under the conditions given in Fig. 2. The simulations were conducted with the model given in the text for a domain diameter $d = 7.8$ and parameter values $a = 0.8$, $\varepsilon = 0.025$, and $b = 0.12$. A black (white) color code denotes large positive (negative) amplitude of the mode, while gray areas lie in the vicinity of zero amplitude.

tion of the spatiotemporal dynamics of these modes yields a wave rotating around the center of the circular domain. In polar coordinates the angular profiles of the nth pair of modes (with indices $2n - 1$ and $2n$) are well approximated by $A_i(r)\sin(n\theta)$ where the radial parts $A_i(r)$ vanish at the center. The frequencies of the coefficients $a_i(t)$ of the first harmonic mode pair also coincide with the main frequency obtained from a Fourier transformation of the local time series of Fig. 2. The comparison of experiment and simulation clearly demonstrates that the experimental data represent rotating waves, whose frequency increases with decreasing domain size. The frequency increase sets in when the domain diameter d becomes comparable to the free spiral wavelength λ in the unbounded medium [see Fig. 1(b)]. The frequency doubles at a d/λ ratio of approximately 0.75.

An increase of the rotational frequency of such a spiral fragment with decreasing system size has already been predicted by a kinematical theory [8] and in the singular perturbation limit of an excitable medium ($\varepsilon \ll 1$) [15]. The present experimental results are more in line with the predictions of the kinematical theory than with the singular limit, where only a very weak effect of the boundary is found. This stems from the fact that they have been measured close to the existence boundary of spirals [3], where the kinematical theory's assumption of weak excitability holds. In order to obtain parameter dependencies away from this limit and in order to investigate the scaling behavior, we performed numerical simulations with a standard model for excitable media [16],

$$\frac{\partial u}{\partial t} = \frac{1}{\varepsilon}\, u(1 - u)\left(u - \frac{v + b}{a}\right) + D\nabla^2 u\,, \quad (1)$$

$$\frac{\partial v}{\partial t} = u - v\,. \quad (2)$$

with this activator (u)–inhibitor (v) model, we simulated spiral waves for varying domain diameters and different values of b while a and ε were kept constant. An excitable medium is realized by a choice of $a < 1$, b positive and small and $\varepsilon \ll 1$ leading to a stable, homogeneous rest state $(u, v) = (0, 0)$. Since the experimental boundaries, the Ti/TiO_2 layers, can be considered to be inert, we implemented zero-flux boundary conditions. As an initial condition, we created a spiral in a large domain and later imposed circular boundaries with varying domain diameter around the original spiral's center of rotation.

A plot of the numerically calculated rotational period τ vs the domain diameter d shown in Fig. 4 reveals that for high excitability ($b = 0.02$, bottom curve) the period decreases only by about 10% with decreasing d, while for b values close to the existence boundary at $b_{\mathrm{crit}} = 0.125$ ($b = 0.12$, top curve) the period decreases to 30% of its saturation value with decreasing domain size. For all parameter values used here, Eqs. (1) and (2) exhibited steadily rotating spirals in the unbounded domain. When decreasing the domain size, spiral meandering [3,16] is found near the onset of the frequency increase, whereas the spirals are restabilized upon further decrease of the domain size, and the rotation center always coincides with the domain center, as already noted by Davydov and Zykov [8]. Even spirals that are initiated off-center drift toward the middle of the domain. Note that the modes extracted from the experimental data are also centered in the same way [see the example in Fig. 3(a)]. If the domain size d is scaled by the free spiral wavelength λ and the period $\tau(d)$ by the spiral period τ_0 in an unbounded medium, the curves for different b almost collapse into a single curve, as evidenced by the inset of Fig. 4.

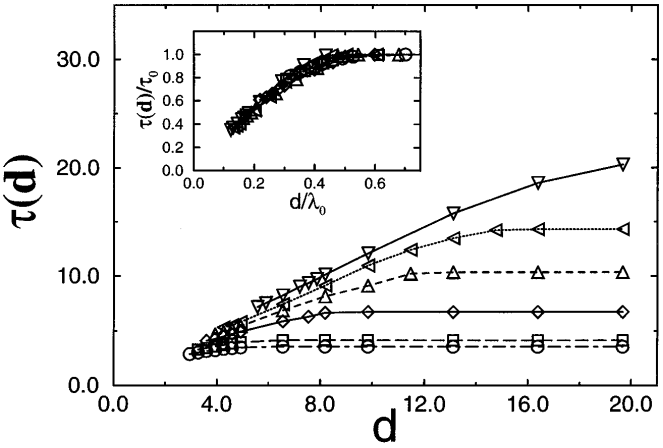

FIG. 4. Simulations showing the dependence of the rotational period τ of spiral waves on the diameter d of circular domains for different parameter values b (from the top to the bottom curve, b values are 0.12, 0.115, 0.11, 0.10, 0.06, and 0.02) at fixed $a = 0.8$ and $\varepsilon = 0.025$. The corresponding wavelength to $b = 0.02$ ($b = 0.12$) is 11.2 (54.2). The inset displays the scaled period τ/τ_0 on the scaled domain diameter d/λ (τ_0 and λ refer to spiral period and wavelength in an unbounded medium).

The simulations support the linear increase of the frequency with the inverse domain size, as anticipated in the analysis of Davydov and Zykov [8]. Figure 4 also shows that the medium below a critical size no longer supports spiral formation. This cutoff length apparently does not scale with the variation of the wavelength; this accounts for the different magnitude of the frequency increase for high excitability (small wavelength comparable to the cutoff length) and low excitability (wavelength larger than the cutoff length). A stability analysis of the spiral waves in a rotating frame [16] with the size as a bifurcation parameter links the cutoff to a saddle-node bifurcation, at which the spiral solution disappears [17].

Simulations and experiment can be discussed in terms of three characteristic quantities: a domain size d_1, below which the frequency starts to increase, a certain domain size d_2, at which the frequency doubles, and finally the cutoff size d_3. While $d_1 > d_3$ in general holds, the relation $d_2 > d_3$, indicating an appreciable change in the rotation

period, is fulfilled only for weak excitability. As shown by the inset of Fig. 4, d_1 and d_2 scale with the spiral wavelength. The scaled values appear to depend on the details of the kinetics since the experiment yields $d_1/\lambda = 1$ and $d_2/\lambda = 0.75$, while the simulation predicts $d_1/\lambda = 0.5$ and $d_2/\lambda = 0.25$.

The increase in the spiral frequency with decreasing domain size can be made plausible with a very simple picture: The restricted boundaries cause a compression of the spiral core, i.e., the quiescent zone in the center of the spiral (visible in Fig. 3 as the gray area in the modes), thus allowing for a faster rotation of the spiral. The compression of the spiral core can be made visible both in experiment and in simulation by making profile cuts through the leading modes (see Fig. 3) of a KL decomposition.

A similar increase in frequency as by reduction of the domain size can also be obtained by the interaction of rotating waves in a small domain. This could be observed under slightly different experimental conditions where the spiral wavelength was about 20 μm in the unbounded medium: In the 20 μm circle, a pair of rotating waves exhibited a 50% lower period than a single rotating wave. On the other hand, in larger circles, wave pairs and single waves rotated with equal frequency. This phenomenon is observed for wave pairs with the same and opposite sense of rotation. Model calculations have already revealed that interaction of rotating waves leads to the formation of bound pairs of waves both in oscillatory [18] and excitable media [19]. In the latter case, a frequency increase analogous to the one seen in our experiment has been reported. This phenomenon is related to the boundary-induced frequency change, since a spiral in the presence of a straight zero-flux boundary can be thought of as interacting with its mirror image.

In summary, we have shown experimentally and in numerical simulations that the properties of spiral waves are decisively influenced in weakly excitable media if the wavelength becomes comparable to the size of the system. Such effects can become important in so-called real heterogeneous catalysts which usually consist of small metal particles and in biological systems where the system size is also often strongly restricted.

We gratefully appreciate financial support by a NATO Collaborative Research Grant (K. K. and I. G. K.), the Deutsche Forschungsgemeinschaft (M. B.) and the National Science Foundation (I. G. K. and M. B.).

*To whom correspondence should be addressed.

[1] A. T. Winfree, Science **175**, 634 (1972); see also; *Chemical Waves and Patterns*, edited by R. Kapral and K. Showalter (Kluwer, Dordrecht, 1994).
[2] P. Devreotes, Science **245**, 1054 (1989); J. Lechleiter, S. Girard, E. Peralta, and D. Clapham, Science **252**, 123 (1991); J. M. Davidenko, A. V. Pertsov, R. Salomonsz, W. Baxter, and J. Jalife, Nature (London) **355**, 349 (1992).
[3] A. T. Winfree, Chaos **1**, 303 (1991); A. S. Mikhailov and V. S. Zykov, Physica (Amsterdam) **52D**, 379 (1991).
[4] K. A. Agladze, J. P. Keener, S. C. Müller, and A. Panfilov, Science **264**, 1746 (1994).
[5] S. C. Müller and V. S. Zykov, in *Dynamical Phenomena in Living Cells*, edited by E. Moseskilde and O. G. Mouritsen (Springer, Berlin, 1995).
[6] J. Selpuchre, and A. Babloyantz, Phys. Rev. E **48**, 187 (1993).
[7] A. M. Pertsov, E. A. Ermakova, and E. E. Shnol, Physica (Amsterdam) **44D**, 178 (1990).
[8] V. A. Davydov and V. S. Zykov, Zh. Eksp. Teor. Fiz. **76**, 414 (1993).
[9] G. Veser and R. Imbihl, J. Chem. Phys. **100**, 8483 (1994).
[10] M. D. Graham, I. G. Kevrekidis, K. Asakura, J. Lauterbach, K. Krischer, H. H. Rotermund, and G. Ertl, Science **264**, 80 (1994).
[11] W. Engel, M. E. Kordesch, H. H. Rotermund, S. Kubala, and A. von Oertzen, Ultramicroscopy **36**, 158 (1991).
[12] E. Lorenz, Massachusetts Institute of Technology, Scientific Report I, 1956, (unpublished); J. L. Lumley, in *The Structure of Turbulence Flow, Atmosphere Turbulence and Radio Progagation*, edited by A. M. Yaglom and V. I. Tatarski (Nauka, Moscow, 1967), p. 166.
[13] L. Sirovich, Q. Appl. Math. **45**, 561 (1987).
[14] K. Krischer, R. Rico-Martínez, I. G. Kevrekidis, H. H. Rotermund, G. Ertl, and J. L. Hudson, AIChE J. **39**, 89 (1993); C. C. Chen, E. E. Wolf, and H.-C. Chang, J. Phys. Chem. **97**, 1055 (1993); A. E. Deane, I. G. Kevrekidis, G. E. Karniadakis, and S. A. Orzsag, Phys. Fluids A **3**, 2337 (1991).
[15] I. S. Aranson, D. Kessler, and I. Mitkov, Phys. Rev. E **50**, R2395 (1994).
[16] D. Barkley, Physica (Amsterdam) **49D**, 61 (1991); Phys. Rev. Lett. **68**, 2090 (1992); Phys. Rev. Lett. **72**, 164 (1994).
[17] A. K. Bangia, M. Bär, and I. G. Kevrekidis (unpublished).
[18] X.-G. Wu, M.-N. Chee, and R. Kapral, Chaos **1**, 421 (1991); I. S. Aranson, L. Kramer, and A. Weber, Phys. Rev. E **47**, 3231 (1993).
[19] E. N. Ermakova, A. M. Pertsov, and E. E. Shnol, Physica (Amsterdam) **40D**, 185 (1989).